1996, after the identification of variant CJD. Additionally, we assumed some degree of BSE underreporting by using maximum estimates of underreporting based on a model of the BSE epidemic published previously (*24*).

12. A positive random variable T is said to have a generalized F distribution with μ and σ as location and scale parameters, respectively, and s_1, s_2, as shape parameters, if $W = [\ln(T) - \mu]/\sigma$ has an F distribution with $2s_1$ and $2s_2$ degrees of freedom. The density of W is given by
$$f(w,s_1,s_2) = \left(\frac{s_1 e^w}{s_2}\right)^{s_1}\left(1 + \frac{s_1 e^w}{s_2}\right)^{-(s_1+s_2)} B(s_1,s_2)^{-1},$$
where $B(x,y)$ is the beta function [i.e., $B(x,y) = \int_0^1 t^{x-1}(1-t)^{y-1}dt$]. The generalized F distribution includes many commonly used distributions as special cases, such as the lognormal, Weibull, gamma, and log-logistic distributions.

13. The quantity $i(s,u|\rho)$ in Eq. 1 can be expressed as
$$i(s,u|\rho) = r(s,u|\rho) \times \exp[-R(s,u|\rho)] \times N(s,u) \quad (2)$$
where $N(s,u)$ is the number of individuals aged u at time s, $r(s,u|\rho)$ is the hazard of infection for these individuals (rate of infection at a given time conditional on having survived uninfected up to that time), and $R(s,u|\rho)$ is the cumulative risk of infection in these individuals up to time s [i.e., $R(s,u) = \int_0^s r(t,u|\rho)dt$]. To take into account variation in exposure/susceptibility to infection with age, the hazard of infection, $r(s,u)$, is allowed to vary with age (u). To estimate the parameters of the model, we must make some assumptions about the way in which $r(s,u)$ varies with age (u). We first made the simplifying assumption that $r(s,u|\rho)$ can be rewritten as $h(s|\rho) \times \phi(u)$; i.e., we assume that the age dependency of the hazard function does not vary over time (likely to be an oversimplification). This would yield the following expression for the distribution of infection over time: $i(s,u|\rho) = h(s|\rho) \times \phi(u) \times \exp[-\phi(u) \times H(s)] \times N(s,u)$, where $H(s)$ stands for the cumulative value of $h(s)$. We further simplified our equation, by approximating the above expression by $i(s,u|r) = h(s) \times \exp[-H(s)] \times k(u) \times N(s,u)$, with $k(u)$ chosen in such a way that the age distribution of cases in the model matches the observed age distribution of cases. In this expression, $h(s)$ was assumed to take the form of a step function [see (*2*)].

14. Supplementary Web material is available on *Science* Online at www.sciencemag.org/cgi/content/full/1064748/DC1.
15. To obtain approximate 95% prediction intervals for the number of cases in a given year, we fitted models in which the annual incidence for that year was fixed, and we compared the likelihood of this model with the maximum likelihood until a log likelihood ratio of 1.92 was obtained.
16. S. E. Lloyd *et al.*, *Proc. Natl. Acad. Sci. U.S.A.* **98**, 6279 (2001).
17. R. I. Carp, R. C. Moretz, M. Natelli, A. G. Dickinson, *J. Gen. Virol.* **68**, 401 (1987).
18. A. Bossers, B. E. Schreuder, I. H. Muileman, P. B. Belt, M. A. Smits, *J. Gen. Virol.* **77**, 2669 (1996).
19. L. Cervenakova *et al.*, *Proc. Natl. Acad. Sci. U.S.A.* **95**, 13239 (1998).
20. K. Manolakou *et al.*, *Proc. Natl. Acad. Sci. U.S.A.* **98**, 7402 (2001).
21. A. R. McLean, C. J. Bostock, *Philos. Trans. R. Soc. London Ser. B* **355**, 1043 (2000).
22. A. Frosh, R. Joyce, A. Johnson, *Br. Med. J.* **322**, 1558 (2001).
23. C. I. Lasmezas *et al.*, *Proc. Natl. Acad. Sci. U.S.A.* **98**, 4142 (2001).
24. R. M. Anderson *et al.*, *Nature* **382**, 943 (1996).
25. This work was supported by the UK Department of Health. The views expressed in this publication are those of the authors and not necessarily those of the UK Department of Health. We thank the Creutzfeldt-Jakob Disease Surveillance Unit and Pr. R. Will for providing the data analyzed in this study.

25 July 2001; accepted 11 October 2001
Published online 26 October 2001;
10.1126/science.1064748
Include this information when citing this paper.

REPORTS

The Influence of the Proinflammatory Cytokine, Osteopontin, on Autoimmune Demyelinating Disease

Dorothée Chabas,[1]* Sergio E. Baranzini,[2]* Dennis Mitchell,[1] Claude C. A. Bernard,[3] Susan R. Rittling,[4] David T. Denhardt,[4] Raymond A. Sobel,[5] Christopher Lock,[1] Marcela Karpuj,[1,2] Rosetta Pedotti,[1] Renu Heller,[6]† Jorge R. Oksenberg,[2]† Lawrence Steinman[1]†‡

Multiple sclerosis is a demyelinating disease, characterized by inflammation in the brain and spinal cord, possibly due to autoimmunity. Large-scale sequencing of cDNA libraries, derived from plaques dissected from brains of patients with multiple sclerosis (MS), indicated an abundance of transcripts for osteopontin (OPN). Microarray analysis of spinal cords from rats paralyzed by experimental autoimmune encephalomyelitis (EAE), a model of MS, also revealed increased OPN transcripts. Osteopontin-deficient mice were resistant to progressive EAE and had frequent remissions, and myelin-reactive T cells in $OPN^{-/-}$ mice produced more interleukin 10 and less interferon-γ than in $OPN^{+/+}$ mice. Osteopontin thus appears to regulate T helper cell–1 (T_H1)–mediated demyelinating disease, and it may offer a potential target in blocking development of progressive MS.

Multiple sclerosis (MS) is often characterized by relapsing episodes of neurologic impairment followed by remissions. In about one-third of MS patients, this disease evolves into a progressive course, termed secondary progressive MS (*1*). In a minority of patients, progressive neurologic deterioration without remission occurs from the onset of disease, and this is called primary progressive MS. The pathophysiologic and genetic causes underlying primary versus secondary progressive MS remain unclear (*2–4*).

Osteopontin, also called early T cell activation gene-1 (*5*, *6*), has pleiotropic functions (*7–9*), including roles in inflammation and in immunity to infectious diseases (*8*). OPN costimulates T cell proliferation (*8*) and is classified as a T helper cell–1 (T_H1) cytokine, because of its ability to enhance interferon-γ (IFN-γ) and interleukin 12 (IL-12) production, and to diminish IL-10 (*10*). We investigated a role for OPN in MS and an experimental model for MS, experimental autoimmune encephalomyelitis (EAE) in mice.

Initially, we set out to identify gene transcripts involved in the inflammatory response that might be increased in the central nervous system (CNS) during active EAE and that returned to normal when EAE was successfully treated after the onset of paralysis. Customized oligonucleotide microarrays were produced to monitor transcription of genes involved in inflammatory responses (*11–14*). These initial microarray experiments showed that osteopontin transcripts were elevated in the brains of rats with EAE but not in brains of rats protected from EAE. Details of these experiments are available at *Science* Online (*14*).

In parallel, we performed high-throughput sequencing of expressed sequence tags (ESTs), using nonnormalized cDNA brain libraries (*15–17*), generated from MS brain lesions and control brain (*18*). Using this protocol, the mRNA populations present in the brain specimens are accurately represented, enabling the quantitative estimation of transcripts and comparisons between specimens (*18*) [Table 1 ,and Web table 1 (*14*)]. Molecular mining of two sequenced libraries and their comparison with a normal brain library, matched for size and tissue type and constructed with an identical protocol, revealed that OPN transcripts were frequently detected and were exclusive to the MS mRNA population, but not found in control brain mRNA (Table 1).

We sequenced more than 11,000 clones

[1]Department of Neurology and Neurological Sciences, Beckman Center for Molecular Medicine, B002, Stanford, CA 94305, USA. [2]Department of Neurology, University of California at San Francisco School of Medicine, San Francisco, CA 94143, USA. [3]Neuroimmunology Laboratory, Department of Biochemistry, La Trobe University, Bundoora, Victoria, 3083 Australia. [4]Department of Cell Biology and Neuroscience, Rutgers University, Piscataway, NJ 08854, USA. [5]Department of Pathology (Neuropathology), Stanford University School of Medicine, Stanford, CA 94305, USA. [6]Roche Bioscience, 3401 Hillview Avenue, Palo Alto, CA 94304, USA.

*These authors contributed equally to this work.
†These senior authors contributed equally to this work.
‡To whom editorial correspondence should be addressed. E-mail: steinman@stanford.edu

from MS libraries 1 and 2, and control libraries [Web fig. 1 (*14*)] and focused our analysis on genes present in both MS libraries, but absent in the control library (*18*). This yielded 423 genes, including 26 novel genes. From those, 54 genes showed a mean fold change of 2.5 or higher in MS libraries 1 and 2 (Table 1). Transcripts for alpha B-crystallin, an inducible heat shock protein, localized in the myelin sheath, and known to be targeted by T cells in MS, were the most abundant transcripts unique to MS plaques (*19*) (Table 1). The next five most abundant transcripts included those for prostaglandin D synthase, prostatic binding protein, ribosomal protein L17, and OPN.

Next we analyzed all genes present in each of the three cDNA libraries and found 330 (seven novel) genes. Based on the clone count of each sequenced gene, a table was constructed with transcripts showing an average fold difference equal to or greater than ±2.00 between MS and control. Forty of these transcripts were divided into three lev-

Table 1. MS-specific gene transcripts. Only genes with a mean fold change of >2.5 are listed. N/A, mapping position is not known. *, Genomic regions that reached nominal criteria of linkage in genome-wide screenings.

Accession #	Gene description	MS1 abundance	MS2 abundance	Average clone count	Cellular function	Genomic location
S45630	Alpha B-crystallin	7	12	9.5	Cell structure/motility	11q22.3-q23.1
M61901	Prostaglandin D synthase	8	7	7.5	Cell signaling/cell communication	9q34.2-34.3
X75252	Prostatic binding protein	6	7	6.5	Cell signaling/cell communication	12q24.1*
X53777	Ribosomal protein L17	10	2	6	Gene/protein expression	18q
X13694	Osteopontin	8	3	5.5	Cell structure/motility/signaling	4q21-q25
AB037797	KIAA1376	6	3	4.5	Unclassified	5
Z19554	Vimentin	4	5	4.5	Cell structure/motility	10p13
X52947	Cardiac gap junction protein	5	3	4	Cell signaling/cell communication	6q21-q23.2*
D17754	DNA binding protein	4	4	4	Gene/protein expression	12q23-24.1*
AF181862	G protein–coupled receptor	2	6	4	Cell signaling/cell communication	16p12
AB018321	ATPase, Na/K transporting, alpha 2 (KIAA0778)	2	6	4	Cell signaling/cell communication	1q21-q23
AF100620	MORF-related gene *X*	1	7	4	Gene/protein expression	Xq22*
AB002363	KIAA0365	1	7	4	Unclassified	19p12
AF072902	Gp130-associated protein (GAM)	6	1	3.5	Unclassified	19p13.3
M11233	Cathepsin D	6	1	3.5	Cell/organism defense	11p15.5
D78014	Dihydropyrimidinase-related protein-3	6	1	3.5	Metabolism	5q32
X53305	Stathmin	4	3	3.5	Cell division	1p36.1-p35*
AF026844	Ribosomal protein L41	4	3	3.5	Unclassified	22q12
U48437	Human amyloid β precursor-like protein 1	4	3	3.5	Unclassified	N/A
U51678	Small acidic protein	3	4	3.5	Unclassified	N/A
U67171	Selenoprotein W	3	4	3.5	Metabolism	19q13.3*
S80794	Tyrosine and tryptophan hydroxylase activator	2	5	3.5	Cell signaling/cell communication	22q12.3
AB011089	KIAA0517 (brain)	4	2	3	Unclassified	4q28
AAD32952	PHR1 isoform 4 [*Mus musculus*]	3	3	3	Unclassified	N/A
J04173	Phosphoglycerate mutase, brain	2	4	3	Metabolism	10q25.3
M22382	Heat shock 60-kD protein 1 (chaperonin)	2	4	3	Cell/organism defense	2
M34671	HUMCD59A Human lymphocytic antigen CD59/MEM43	2	4	3	Unclassified	11p13
M64786	Similar to Myc	2	4	3	Unclassified	N/A
AJ132695	*Rac1* gene	2	4	3	Cell signaling/cell communication	Xq26.2-27.2
Z99716	Septin 3	1	5	3	Cell division	22q13.1
U49436	Human translation initiation factor 5	1	5	3	Gene/protein expression	14q32*
CAA63354	Cysteine string protein [*Bos taurus*]	2	3	2.5	Unclassified	N/A
U90915	Cytochrome c oxidase subunit IV	4	1	2.5	Metabolism	16q24.1
J02611	Apolipoprotein D	4	1	2.5	Metabolism	3q26.2-qter
X05607	Cystatin C (cysteine proteinase inhibitor precursor)	4	1	2.5	Metabolism	20p11.2
U45976	Clathrin assembly protein lymphoid myeloid leukemia	4	1	2.5	Unclassified	11q14
J00272	Metallothionein-II pseudogene	4	1	2.5	Unclassified	4p11-q21
S69965	β-Synuclein	3	2	2.5	Unclassified	5q35
Y00711	Lactate dehydrogenase B	3	2	2.5	Metabolism	12p12.2-p12.1
L37033	FX-506 binding protein homolog (FKBP38)	3	2	2.5	Cell signaling/cell communication	19p12
AF044956	NADH:ubiquinone oxidoreductase B22 subunit	3	2	2.5	Metabolism	8q13.3
AB011154	KIAA0582 (brain)	3	2	2.5	Unclassified	2p12
X55039	Centromere autoantigen B	3	2	2.5	Unclassified	20p13
X64364	Basigin	3	2	2.5	Cell signaling/cell communication	19p13.3
U82761	*S*-Adenosyl homocysteine hydrolase-like 1	3	2	2.5	Metabolism	1
D13627	Chaperonin-containing TCP1, subunit 8 (theta)	2	3	2.5	Gene/protein expression	21q22.11
Z47087	Transcription elongation factor B (SIII), polypeptide 1-lik	2	3	2.5	Gene/protein expression	5q31
X75861	Testis enhanced gene transcript	2	3	2.5	Cell division	12q12-q13
M16447	Quinoid dihydropteridine reductase	2	3	2.5	Metabolism	4p15.31
M22918	Nonmuscle myosin alkali light chain	2	3	2.5	Unclassified	12
M55270	Matrix Gla protein	2	3	2.5	Unclassified	12p13.1-p12.3
AF151807	CGI-49 protein	2	3	2.5	Unclassified	1
AAD45960	Human EST H08032.1 (NID:g872854)	2	3	2.5	Unclasified	7q11.23-q21.1

els, on the basis of the consistency of differential expression across libraries [Web table 1 (*14*)]. Some of these genes [Web table 1 (*14*)] were myelin basic protein (MBP), heat shock protein 70 (HSP-70), glial fibrillary acidic protein (GFAP), and synaptobrevin. MBP transcripts displayed consistent high levels of expression in the three libraries, suggesting a very high turnover rate for this protein. Expression of HSP70, which is involved in myelin folding (*20*), was significantly elevated. Although not differentially expressed, GFAP was among the three most abundant species in all the libraries, consistent with a prominent glial (or astrocytic) response in the MS brains. Six genes belonging to the KIAA group of large-size cloned mRNAs showed differential expression. The decreased transcription of synaptobrevin might be of interest, given that it belongs to a family of small integral membrane proteins specific for synaptic vesicles in neurons. Recent evidence indicates that axonal loss is one of the major components of pathology in MS (*21*, *22*).

Given the known inflammatory role for OPN, we examined the cellular expression pattern of this protein in human MS plaques and in control tissue, by immunohistochemistry. To identify cells expressing OPN in situ, we used a polyclonal antibody, generated in mouse against recombinant glutathione *S*-transferase (GST)–OPN, to stain postmortem MS and control tissue samples (*23*) (Fig. 1, A and B). Within active MS plaques, OPN was found on microvascular endothelial cells and macrophages (Fig. 1A), and in white matter adjacent to plaques. Reactive astrocytes and microglia also expressed OPN (Fig. 1B).

The role of OPN in inflammatory demyelinating disease was next examined by using two models of EAE (*1*). A relapsing-remitting model of EAE was first used to compare the cellular expression of OPN at different stages of the disease. Disease was induced in SJL mice by immunization with the proteolipid protein peptide 139–151 (PLP 139-151) in complete Freund's adjuvant (CFA), and the animals were scored daily for signs of disease (*24*). Brain and spinal cord were removed during acute phase, remission, or first relapse (*25*). Histopathologic identification of OPN in EAE was then performed (Fig. 1, C to F). OPN was expressed broadly in microglia during both relapse and remission from disease, and this expression was focused near perivascular inflammatory lesions. In addition to OPN expression on glia, expression in neurons was detectable during acute disease and relapse, but not during remission. To confirm the expression of OPN in an acute form of EAE, a rapid, monophasic demyelinating disease was induced in Lewis rats (*12*), then OPN immunostaining was performed on their brains (Fig. 1G) (*29*). OPN expression in microglia and neurons was predominant in the sick rats and was focused close to the acute lesions, as was observed in the relapsing-remitting mouse model of EAE. Staining of OPN in bone with the same antibody, MPIIIB10$_1$, served as a positive control (Fig. 1H). These results strongly implicated OPN in acute, as well as in relapsing, forms of EAE and suggested that the degree of expression of OPN in lesions correlated with the severity of disease.

The potential role of OPN in demyelinating disease was next tested using OPN-deficient mice (Fig. 2) (*30*). EAE was induced by using myelin oligodendrocyte glycoprotein peptide 35–55 (MOG 35-55) in CFA in OPN$^{-/-}$ mice and OPN$^{+/+}$ controls (*31*). EAE was observed in 100% of both OPN$^{+/+}$ and OPN$^{-/-}$ mice with MOG 35-55. Despite this, severity of disease was significantly reduced in all animals in the OPN$^{-/-}$ group (Fig. 2A), and these mice were totally protected from EAE-related death (Fig. 2B). Thus, OPN significantly influenced the course of progressive EAE induced by MOG 35-55.

The rate of relapses and remissions was next tested. During the first 26 days, OPN$^{-/-}$ mice displayed a distinct evolution of EAE, with a much higher percentage of mice having remissions compared with the controls (Fig. 2C). OPN$^{+/+}$ and OPN$^{-/-}$ mice were killed on days 28, 48, and 72 after immunization for histopathology. Although the clinical courses in the two groups were quite different, there were similar numbers and appearances of inflamma-

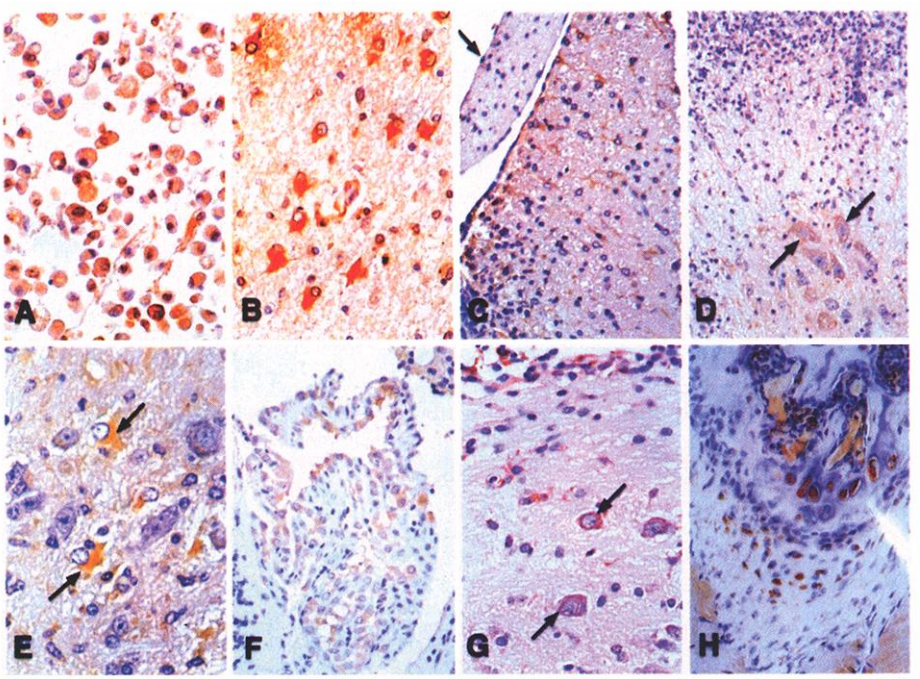

Fig. 1. CNS expression of osteopontin in demyelinating disease. (**A** and **B**). MS in humans. OPN in macrophages in the center of an actively demyelinating MS plaque (A) and in white matter astrocytes adjacent to an active MS plaque (B). OPN staining was performed with a polyclonal antibody against OPN on paraffin-embedded sections. (**C** to **F**) Relapsing-remitting EAE in mice. EAE was induced in nine SJL mice (The Jackson Laboratory, Bar Harbor, ME) with PLP 139-151, as previously described (*24*). Four mice injected with PBS served as controls. Immunostaining was performed with the antibody against OPN, MPIIIB10$_1$ (Developmental Studies Hybridoma Bank, Iowa City, IA) (*25*), and slides were examined by an observer blinded to the experimental design. (C) OPN was broadly expressed in CNS microglia, especially near inflammatory lesions, but not in adjacent peripheral nerves (arrow). (D) Expression in neurons (arrows) was detectable during the acute phase (n = 4) and relapse (n = 2), but not during remission (n = 1) or in mice with inflammatory lesions that never developed paralysis (n = 2). (E) OPN expression in astrocytes (arrows) and choroid plexus cells (F) was also more frequent and more pronounced in immunized mice (100%) than in controls (25%). (**G**) Acute EAE in rat. EAE was induced in 19 Lewis rats (The Jackson Laboratory) as described in (*13*) but with 400 μg guinea pig spinal cord homogenized in complete Freund's adjuvant (GPSCH). Four rats injected with CFA alone served as controls. Brains were processed and stained with MPIIIB10$_1$ (*29*). Microglial expression of OPN around inflammatory lesions (G) correlated with the clinical disease severity. OPN was also expressed in neurons (arrows), mostly in the animals with severe clinical signs. (**H**) Positive control. OPN staining in the bony growth plate of a mouse femur with MPIIIB10$_1$. All photos are immunoperoxidase-stained with diaminobenzidine chromogen and hematoxylin counterstain. Magnifications: (A–D, F, and H), ×370; (E and G), ×494.

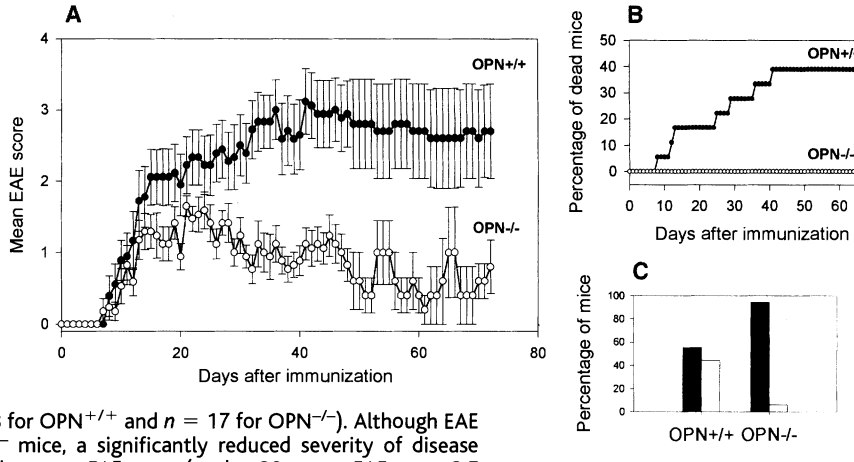

Fig. 2. Clinical attenuation of EAE in OPN$^{-/-}$ mice. (**A**) EAE was induced in OPN$^{+/+}$ (n = 18) (closed circles) and OPN$^{-/-}$ (n = 17) (open circles) mice (*30*) with MOG 35-55, as described in (*31*). EAE was scored as follows: 0, normal; 1, monoparesis; 2, paraparesis; 3, paraplegia; 4, tetraparesis; and 5, moribund or dead. For each animal, a remission was defined by a decrease of the score of at least one point for at least two consecutive days. EAE was considered remitting when at least one remission occurred within the first 26 days, and progressive when no remission occurred. OPN$^{-/-}$(open circles) mice have milder disease than OPN$^{+/+}$ controls (closed circles). The error bars represent the standard error for each point. EAE was observed in 100% of both OPN$^{+/+}$ and OPN$^{-/-}$ mice treated with MOG 35-55 to induce EAE (n = 18 for OPN$^{+/+}$ and n = 17 for OPN$^{-/-}$). Although EAE could be induced with a 100% incidence in OPN$^{-/-}$ mice, a significantly reduced severity of disease developed in the OPN$^{-/-}$ group, with a decrease of the mean EAE score (at day 30, mean EAE score 2.5 in OPN$^{+/+}$ compared with 1.2 in OPN$^{-/-}$; Mann-Whitney rank sum test; P = 0.0373) and a decrease of the mean maximum severity score (mean severity 3.7 in OPN$^{+/+}$ compared with 2.8 in OPN$^{-/-}$; Mann-Whitney rank sum test; P = 0.0422) . There was no significant delay of the day of onset of disease (mean 11.7 days in OPN$^{+/+}$ compared with 12.5 days in OPN$^{-/-}$; Mann-Whitney rank sum test; P = 0.322). (**B**) OPN$^{-/-}$ mice (open circles) are protected from EAE-related death: 0 dead out of 17 compared with 7 dead out of 18 in the OPN$^{+/+}$ mice at day 70 (P = 0.0076 by Fisher's exact test). (**C**) OPN promotes progressive EAE. The bars represent the percentage of mice having a remitting (black) or progressive (white) disease in each group. OPN$^{-/-}$ mice showed a distinct evolution of EAE, with a much higher percentage of mice having remissions compared with the controls. Ten out of 18 had remissions in the OPN$^{+/+}$ group (55.5%) compared with 16 out of 17 in the OPN$^{-/-}$ group (94.1%) (P = 0.0178 by Fisher's exact test).

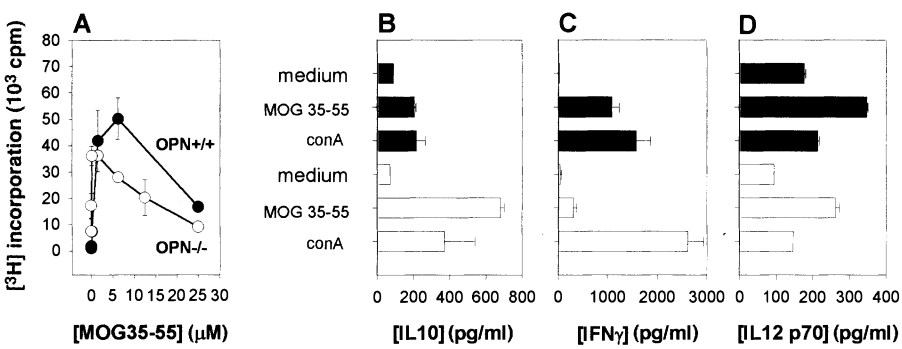

Fig. 3. Attenuated T cell activation by MOG 35-55 in OPN$^{-/-}$ mice. (**A**) Inhibition of T cell proliferation in OPN$^{-/-}$ mice. A proliferation assay was performed on draining lymph nodes (LNs) from OPN$^{+/+}$ (closed circles) and OPN$^{-/-}$ (open circles) mice (*30*), 14 days after induction of EAE. EAE was induced with MOG 35-55, as described in (*31*). Draining LNs were removed 14 days after immunization, and LN cells were stimulated in 96-well flat-bottom plates (2.5 × 10^6/ml, 200 μl/well) with serial dilutions of MOG 35-55 (0-50 μM) purified by high-performance liquid chromatography, as described (*39*). The medium contained 2% serum from the type of mouse tested, in order to avoid introducing OPN into the in vitro assays on OPN$^{-/-}$ cells: OPN$^{+/+}$ normal mouse serum was used for the assays on OPN$^{+/+}$ cells; OPN$^{-/-}$ normal mouse serum was used for the assays on OPN$^{-/-}$ cells. Concanavalin A (2 μg/ml), a nonspecific mitogen for T cells, was used as a nonspecific positive control. [^{3}H]Thymidine was added to the triplicates (mean ± SD graphed), after 72 hours of antigen stimulation, and its incorporation by the proliferating cells (in counts per minute) was measured 24 hours later. (**B**) OPN$^{-/-}$ cells produce more IL-10 than OPN$^{+/+}$ cells. OPN$^{+/+}$ (black bars) and OPN$^{-/-}$ (white bars) LN cells were stimulated in the same way as for the proliferation assay (Fig. 3A), but in 24-well flat-bottom plates (2 ml/well). MOG 35-55 was used at a concentration of 12.5 μM. IL-10 was measured by ELISA on the 48-hour supernatants (dilution 1/2), in duplicate (mean ± SD graphed), according to the manufacturer's instructions. (**C**) OPN$^{-/-}$ cells produce less IFN-γ than OPN$^{+/+}$ cells. OPN$^{+/+}$ (filled bars) and OPN$^{-/-}$ (open bars) spleen cells were removed 14 days after induction of EAE with MOG 35-55 and stimulated as described for Fig. 3B, but with 4.5 × 10^6 cells/well. IFN-γ was measured by ELISA on the 48-hour supernatants (dilution 1/5), in triplicate, according to the manufacturer's instructions. (**D**) OPN$^{-/-}$ cells produce less IL-12 than OPN$^{+/+}$ cells. OPN$^{+/+}$ (black bars) and OPN$^{-/-}$ (white bars) spleen cells were removed as described for Fig. 3C. IL-12 p70 was measured by ELISA on the 24-hour supernatants (dilution 1/1), in duplicate (mean ± SD graphed), according to the manufacturer's instructions (OPTEIA kit, PharMingen, San Diego, CA).

tory foci within the CNS (*32*). Therefore, although OPN may not influence the extent of the inflammatory response, this molecule might critically influence whether the course of disease is progressive, or whether relapses and remissions develop.

To examine whether different immune responses were involved in OPN$^{-/-}$ and OPN$^{+/+}$ animals, we tested the profile of cytokine expression in these mice. Because EAE is a T cell–mediated disease, we first analyzed the T cell proliferative response to the autoantigen MOG 35-55 in the OPN$^{-/-}$ mice. T cells in OPN$^{-/-}$ mice showed a reduced proliferative response to MOG 35-55, compared with OPN$^{+/+}$ T cells (Fig. 3A). In addition, IL-10 production was increased in T cells reactive to MOG 35-55 in OPN$^{-/-}$ mice that had developed EAE, compared with T cells in OPN$^{+/+}$ mice (Fig. 3B). At the same time, IFN-γ and IL-12 production was diminished in the cultures of spleen cells stimulated with MOG (Fig. 3, C and D).

Because IFN-γ and IL-12 are important proinflammatory cytokines in MS (*1*, *33*), the finding that in OPN$^{-/-}$ mice there is reduced production of these cytokines is consistent with the hypothesis that OPN may play a critical role in the modulation of T_H1 immune responses in MS and EAE. Further, IL-10 has been associated with remission from EAE (*34*). In this context, the enhancement of myelin-specific IL-10 production in OPN$^{-/-}$ mice may account for the tendency of these mice to go into remission. Sustained expression of IL-10 may thus be an important factor in the reversal of relapsing MS, and its absence may allow the development of secondary progressive MS.

In conclusion, our data support the idea that OPN may have pleiotropic functions in the pathogenesis of demyelinating disease. OPN production by glial cells may lead to the attraction of T_H1 cells, and its presence in glial and ependymal cells may allow inflammatory T cells to penetrate the brain. Finally, our data suggest that neurons may also secrete this proinflammatory molecule and par-

ticipate in the autoimmune process. Potentially, neuronal OPN secretion could modulate inflammation and demyelination and could influence the clinical severity of the disease. Consistent with this idea, a role for neurons in the pathophysiology of MS and EAE has recently been described (*21*, *22*), and neurons are known to be capable of cytokine production (*35*, *36*). OPN inhibits cell lysis (*6*), and thus, neuronal OPN might even protect the axon from degeneration during autoimmune demyelination.

CD44 is a known ligand of OPN, mediating a decrease of IL-10 production (*10*). As shown here, $OPN^{-/-}$ mice produced elevated IL-10 during the course of EAE. We recently demonstrated that antibodies against CD44 prevented EAE (*37*), suggesting that the proinflammatory effect of OPN in MS and EAE might be mediated by CD44. The binding of OPN to its integrin fibronectin receptor $\alpha_V \beta_3$ through the arginine-glycine-aspartate tripeptide motif may also perpetuate T_H1 inflammation (*10*). In active MS lesions, the α_V subunit of this receptor is overexpressed in macrophages and endothelial cells, and the β_3 subunit is expressed on endothelial cell luminal surfaces (*23*). By means of its tripeptide-binding motif, OPN inhibits inducible nitric oxide synthetase (iNOs) (*38*), which is known to participate in autoimmune demyelination (*1*). Thus, in conclusion, OPN is situated at a number of checkpoints that would allow diverse activities in the course of autoimmune-mediated demyelination.

References and Notes

1. L. Steinman, *Nature Immunol.* **2**, 762 (2001).
2. J. L. Haines *et al.*, *Nature Genet.* **13**, 469 (1996).
3. G. C. Ebers *et al.*, *Nature Genet.* **13**, 472 (1996).
4. S. Sawcer *et al.*, *Nature Genet.* **13**, 464 (1996).
5. A. Oldberg, A. Franzen, D. Heinegard, *Proc. Natl. Acad. Sci. U.S.A.* **83**, 8819 (1986).
6. L. W. Fisher *et al.*, *Biochem. Biophys. Res. Commun.* **280**, 460 (2001).
7. D. T. Denhardt, X. Guo, *FASEB J.* **7**, 1475 (1993).
8. A. W. O'Regan *et al.*, *Immunol. Today* **21**, 475 (2000).
9. S. R. Rittling, D. T. Denhardt, *Exp. Nephrol.* **7**, 103 (1999).
10. S. Ashkar *et al.*, *Science* **287**, 860 (2000).
11. The custom microarray has 517 genes, with 60 probe pairs per gene, and a feature size of 50 × 50 micrometers. Rat, mouse, and human genes for cytokines, chemokines, bone growth factors, proteases, and molecules related to cell death are included on this chip.
12. N. Karin *et al.*, *J Immunol.* **160**, 5188 (1998).
13. K. Gijbels, R. E. Galardy, L. Steinman, *J. Clin. Invest.* **94**, 2177 (1994).
14. Rats were treated with 75 mg/kg body weight per day orally of the MMP inhibitor RS110379, from day 10 to day 16, and killed on day 16. Further information on this experiment (as well as details of the analysis of transcripts with custom microarrays, Web fig. 1, and Web table 1), is available as supplementary material on *Science* Online at www.sciencemag.org/cgi/content/full/294/5547/1731/DC1.
15. K. G. Becker *et al.*, *J. NeuroImmunol.* **77**, 27 (1997).
16. S. S. Choi *et al.*, *Mamm. Genome* **6**, 653 (1995).
17. N. Sasaki *et al.*, *Genomics* **49**, 167 (1998).
18. In contrast to normalized libraries in which high-frequency transcripts are preferentially eliminated by nuclease treatment of DNA-RNA hybrids to facilitate detection of rare RNA species, we produced nonnormalized libraries, where manipulation of clones is avoided. White matter brain tissue from the plaques of three MS patients was collected and frozen within 2 hours after death. Patient history on the specimen used for the first library (herein MS1) included clinically definite MS and the presence of active inflammatory lesions. Material for the second MS library (herein MS2) came from a pool of tissues from two patients, one with acute, active lesions and widespread inflammatory involvement in the white matter, and the other with chronic, "silent" lesions, with gliosis, but without evidence of a lymphocytic infiltrate. The control library (CTRL) was constructed using pooled mRNA isolated from midbrain white matter, inferior temporal cortex, medulla, and posterior parietal cortex tissue removed from a 35-year-old Caucasian male who died from cardiac failure and who had no neuropathological changes. Details of construction of the libraries can be found as supplementary material on *Science* Online, particularly in the legends to Web fig. 1 and Web table 1 (*14*).
19. J. M. van Noort *et al.*, *Nature* **375**, 798 (1995).
20. D. A. Aquino *et al.*, *Neurochem. Res.* **23**, 413 (1998).
21. D. Pitt, P. Werner, C. S. Raine, *Nature Med.* **6**, 67 (2000).
22. B. D. Trapp *et al.*, *N. Engl. J. Med.* **338**, 278 (1998).
23. R. A. Sobel *et al.*, *J. Neuropathol. Exp. Neurol.* **54**, 202 (1995).
24. R. Pedotti *et al.*, *Nature Immunol.* **2**, 216 (2001).
25. Mice were killed during relapse and remission and perfused with 60 ml of 10% formalin. Brain and spinal cord were removed and fixed in the same solution. Paraffin sections (6 to 10 μm) were prepared. OPN was detected with the monoclonal antibody against OPN, $MPIIIB10_1$ (Developmental Studies Hybridoma Bank, Iowa City, IA), at 1/50 dilution, using the Vector Mouse on Mouse (M.O.M.) immunodetection kit (Vector Laboratories, catalog no. PK 2200), the Vectastain Elite ABC kit (Vector Laboratories, catalog no. PK 6100), according to the manufacturer's instructions, and the substrate 3,3′-diaminobenzidine (0.5 mg/ml for 4 min). The intensity of the cellular staining was evaluated by an observer blinded to the experimental design according to a semiquantitative scale (three grades). $MPIIIB10_1$ stains OPN in immunohistochemical sections from mice, although it does not recognize OPN on Western blots (*26*). The successful use of $MPIIIB10_1$ in mouse sections has been reported (*27*, *28*).
26. S. R. Rittling, F. Feng, *Biochem. Biophys. Res. Commun.* **250**, 287 (1998).
27. N. Dorheim *et al.*, *J. Cell Phys.* **154**, 317 (1993).
28. C. Grainger, *Nature Med.* **1**, 1063 (1995).
29. Details of immunohistochemical staining were performed as described in the supplementary material on *Science* Online (*14*).
30. S. R. Rittling, *et al.*, *J. Bone Miner. Res.* **13**, 1101 (1998).
31. A. Slavin *et al.*, *Autoimmunity* **28**, 109 (1998).
32. $OPN^{+/+}$ and $OPN^{-/-}$ mice are 129/C57BL/6 mixed background, maintained as a partially outbred strain (*30*). Induction of EAE is described further as supplementary information on *Science* Online (*14*).
33. L. Steinman, *Cell* **85**, 299 (1996).
34. M. K. Kennedy *et al.*, *J. Immunol.* **149**, 2496 (1992).
35. H. Villarroya *et al.*, *J. Neurosci. Res.* **49**, 592 (1997).
36. S. L. Shin *et al.*, *Neurosci. Lett.* **273**, 73 (1999).
37. S. Brocke *et al.*, *Proc. Natl. Acad. Sci. U.S.A.* **96**, 6896 (1999).
38. S. M. Hwang *et al.*, *J. Biol. Chem.* **269**, 711 (1994).
39. P. J. Ruiz *et al.*, *J. Immunol.* **162**, 3336 (1999).

40. High-throughput EST sequencing was performed in collaboration with Incyte Genomics. We thank B. Romagnolo for her outstanding help when setting up the breeding of the mice and her statistical expertise and J. Eaton for her technical support. We thank the NIH, the National Multiple Sclerosis Society, the Susan G. Komen Breast Cancer Foundation, the Association Française Contre les Myopathies, the Ligue Française Contre la Sclérose en Plaques, and the Assistance Publique des Hopitaux de Paris for support.

30 May 2001; accepted 15 October 2001

Priming of Memory But Not Effector CD8 T Cells by a Killed Bacterial Vaccine

Gregoire Lauvau,[1]* Sujata Vijh,[2]*† Philip Kong,[2] Tiffany Horng,[2] Kristen Kerksiek,[2]‡ Natalya Serbina,[1] Roman A. Tuma,[1] Eric G. Pamer[1]§

Killed or inactivated vaccines targeting intracellular bacterial and protozoal pathogens are notoriously ineffective at generating protective immunity. For example, vaccination with heat-killed *Listeria monocytogenes* (HKLM) is not protective, although infection with live *L. monocytogenes* induces long-lived, CD8 T cell–mediated immunity. We demonstrate that HKLM immunization primes memory CD8 T lymphocyte populations that, although substantial in size, are ineffective at providing protection from subsequent *L. monocytogenes* infection. In contrast to live infection, which elicits large numbers of effector CD8 T cells, HKLM immunization primes T lymphocytes that do not acquire effector functions. Our studies show that it is possible to dissociate T cell–dependent protective immunity from memory T cell expansion, and that generation of effector T cells may be necessary for long-term protective immunity.

CD8 T lymphocytes mediate immunity to a broad range of viral, bacterial, and protozoal pathogens (*1*), and increasing evidence suggests that effector T cells primed during infection evolve into long-lived memory cells (*2*–*4*). Memory T cells can be subdivided into two categories on the basis of activation markers, homing receptor expression, and effector function (*5*). Central memory T cells, which express high levels of the chemokine